IRSTI 29.51.21 https://doi.org/10.51889/IJAPA.2026.1.1.001

A MINIMAL NEWTONIAN MODEL FOR WHITE DWARFS WITH DARK MATTER ADMIXTURE

A. Muratkhan[1], **N. Shynggyskhan**[1] **and S. Toktarbay**[1*]

[1] *Al-Farabi Kazakh National University, Almaty, Kazakhstan*

*Corresponding Author: saken.toktarbay@kaznu.edu.kz

Received 18 May 2026; Accepted 30 May 2026

Abstract. We consider a simple Newtonian model of a non-rotating white dwarf containing a dark-matter admixture. The baryonic component is described by the Chandrasekhar equation of state for a cold degenerate electron gas, whereas the dark component is modeled as an independent polytropic fluid. The two components are coupled only through the common Newtonian gravitational field. Numerical solutions are constructed for a reference baryonic sequence and for representative mixed configurations with fixed dark-sector parameters. Attention is restricted to three basic outputs: the density profiles, the mass–radius relation, and the limiting mass readout within the explored density interval. At $\rho_{b,c} = 10^8$ g cm^{-3}, the representative mixed models reduce the total mass by about 14.08% for $\delta = 0.25$ and by about 19.17% for $\delta = 0.35$, relative to the purely baryonic configuration. The goal is not to identify a specific dark-matter particle model, but to provide a transparent baseline calculation showing how an additional gravitating component can modify the equilibrium sequence of white dwarfs.

Keywords: white dwarfs; dark matter admixture; Newtonian gravity; Chandrasekhar equation of state; mass–radius relation.

1. INTRODUCTION

The nature of dark matter remains one of the central open problems in modern astrophysics and cosmology. Although its existence is supported by a broad range of gravitational observations, its microscopic properties are still unknown [1, 2, 3]. For this reason, compact astrophysical objects are often used as theoretical laboratories for testing whether a dark component can leave observable or structural signatures in self-gravitating systems [4, 5, 6].

Among compact stars, white dwarfs are especially suitable for baseline studies. Their equilibrium structure is well understood in Newtonian gravity through the Chandrasekhar model, where electron degeneracy pressure supports the star against gravitational collapse [7, 8, 9, 10, 11, 12]. This makes white dwarfs a natural reference system for asking a simple and physically meaningful question: how does the presence of an additional dark matter component modify the standard baryonic configuration?

Dark matter effects in compact stars have been discussed in different contexts, including neutron stars, mixed compact objects, and self-gravitating dark-sector configurations [4, 5, 6]. However, much of the existing literature is focused either on relativistic stars, on model-dependent dark-sector interactions, or on scenarios with more complicated microphysics. In contrast, there is still value in constructing a minimal and transparent Newtonian benchmark for white dwarfs with dark matter admixture. Such a model can clarify the basic structural trends, provide a clean point of comparison with the standard Chandrasekhar sequence, and serve as a starting point for later extensions. Dark-matter-admixed white dwarfs have been investigated in several related contexts [13, 14, 15, 16, 17]. Leung et al. studied white dwarfs containing degenerate fermionic dark-matter cores and showed that sufficiently light dark matter can significantly reduce the stellar radius and the Chandrasekhar mass limit [13]. More recent relativistic two-fluid studies have further demonstrated that light fermionic dark

matter may modify the compactness and radial stability properties of white dwarfs [15]. Other approaches have incorporated cold dark matter into hot-white-dwarf equations of state or have adopted a single-fluid treatment of the baryonic and dark components [17]. These works indicate that even a modest dark component can produce measurable structural changes in white-dwarf configurations.

The purpose of the present work is complementary. Instead of adopting a specific particle-physics model or a fully relativistic formulation, we construct a minimal Newtonian two-component benchmark in which the baryonic sector is described by the Chandrasekhar equation of state and the dark sector by an effective polytropic equation of state. This formulation allows us to isolate the equilibrium role of dark matter admixture, to compare directly with the standard Chandrasekhar sequence, and to distinguish the baryonic radius from the full spatial extent of the mixed configuration.

In the present work, we consider a non-rotating, spherically symmetric white dwarf containing both baryonic matter and a dark matter component. The two sectors are treated as fluids coupled through the common gravitational potential. The baryonic matter is described by the Chandrasekhar equation of state, while the dark matter component is modeled with an independent equation of state [7, 10, 12, 13].

The paper is organized as follows. Section 2. introduces the two-component model and the equations of state. Section 3. summarizes the numerical scheme and the global quantities extracted from the solutions. Section 4. presents the main results. Final remarks and limitations are collected in Section 5..

2. NEWTONIAN TWO-COMPONENT MODEL

We consider a cold, non-rotating, spherically symmetric white dwarf composed of a baryonic component and a dark matter component. Both fluids move in the same Newtonian gravitational potential. The total mass density is therefore written as

$$\rho_{tot}(r) = \rho_b(r) + \rho_{dm}(r), \tag{1}$$

where ρ_b and ρ_{dm} denote the baryonic and dark-matter densities, respectively. The enclosed total mass satisfies

$$\frac{dm}{dr} = 4\pi r^2 \left[\rho_b(r) + \rho_{dm}(r)\right]. \tag{2}$$

Hydrostatic equilibrium for the two components is then described by

$$\frac{dp_b}{dr} = -\rho_b \frac{Gm(r)}{r^2}, \tag{3}$$

$$\frac{dp_{dm}}{dr} = -\rho_{dm} \frac{Gm(r)}{r^2}. \tag{4}$$

In other words, the two fluids are coupled only through their common gravitational field. No direct non-gravitational interaction is included.

2.1. Baryonic equation of state

The baryonic component is described by the zero-temperature Chandrasekhar equation of state, with the standard zero-temperature electron-gas formulation and related refinements [7, 9, 18]. Introducing the relativity parameter

$$x = \frac{p_F}{m_e c}, \tag{5}$$

where p_F is the electron Fermi momentum, one can write the pressure and density as

$$p_b(x) = K\left[x(2x^2-3)\sqrt{1+x^2}+3\sinh^{-1}(x)\right], \tag{6}$$

$$\rho_b(x) = \rho_0 x^3. \tag{7}$$

The constants are

$$K = \frac{\pi m_e^4 c^5}{3h^3}, \qquad \rho_0 = \frac{8\pi\mu_e m_u (m_e c)^3}{3h^3}, \tag{8}$$

where m_e is the electron mass, m_u is the atomic mass unit, h is Planck's constant, c is the speed of light, and μ_e is the mean molecular weight per electron. In the numerical calculations we set $\mu_e = 2$, appropriate for a carbon–oxygen white dwarf.

2.2. Dark matter equation of state

The dark component is modeled phenomenologically as a polytropic fluid,

$$p_{dm} = K_{dm}\rho_{dm}^{\gamma}, \tag{9}$$

where K_{dm} is the polytropic constant and γ is the effective adiabatic index. Polytropic models are widely used as effective descriptions of self-gravitating fluids, including compact-star applications [19, 20, 21, 22, 23]. This form is introduced only as an effective description; it is not intended to select a unique microscopic dark-matter model.

For the numerical calculations presented here, the dark-sector parameters are fixed to

$$\gamma = \frac{5}{3}, \qquad \alpha = \frac{K_{dm}\rho_0^{\gamma}}{K} = 1. \tag{10}$$

With this choice, the dark component is represented by a single reference polytropic law whose dimensionless pressure scale is tied to the Chandrasekhar normalization. The aim of this choice is deliberately restricted: it provides a controlled setup in which the structural effect of an additional self-gravitating component can be isolated.

2.3. Central conditions and radii

At the center we impose

$$m(0) = 0, \qquad \rho_b(0) = \rho_{b,c}, \qquad \rho_d m(0) = \rho_{dm,c}. \tag{11}$$

The central admixture parameter is defined by

$$\delta = \frac{\rho_{dm,c}}{\rho_{b,c}}. \tag{12}$$

The limit $\delta = 0$ reduces the system to the standard baryonic white-dwarf sequence.

The baryonic radius is defined through

$$p_b(R_b) = 0, \tag{13}$$

or, equivalently, by the condition $x(R_b) = 0$. The dark-matter radius is defined by

$$p_{dm}(R_{dm}) = 0. \tag{14}$$

The total radial extent is

$$R = \max(R_b, R_{dm}). \tag{15}$$

In what follows, R_b is used as the main stellar radius because it marks the outer boundary of the visible baryonic matter.

2.4. Dimensionless equations used in the integration

For the numerical integration it is convenient to introduce the Chandrasekhar scales

$$a = \left(\frac{K}{4\pi G\rho_0^2}\right)^{1/2}, \qquad m_0 = 4\pi\rho_0 a^3, \tag{16}$$

and the dimensionless variables

$$r = a\bar{r}, \qquad m = m_0\bar{m}, \qquad \rho_b = \rho_0 x^3, \qquad \rho_{dm} = \rho_0 y. \tag{17}$$

The dimensionless dark-sector stiffness is

$$\alpha = \frac{K_{dm}\rho_0^{\gamma}}{K}. \tag{18}$$

Defining

$$\phi(x) = x(2x^2-3)\sqrt{1+x^2} + 3\sinh^{-1}(x), \tag{19}$$

the coupled system becomes

$$\frac{d\bar{m}}{d\bar{r}} = \bar{r}^2(x^3+y), \tag{20}$$

$$\frac{dx}{d\bar{r}} = -\frac{\bar{m}x^3}{\bar{r}^2}\left(\frac{d\phi}{dx}\right)^{-1}, \tag{21}$$

$$\frac{dy}{d\bar{r}} = -\frac{\bar{m}}{\alpha\gamma\bar{r}^2}y^{2-\gamma}, \qquad y > 0. \tag{22}$$

The corresponding central values are

$$x(0) = x_c = \left(\frac{\rho_{b,c}}{\rho_0}\right)^{1/3}, \qquad y(0) = \delta x_c^3, \qquad \bar{m}(0) = 0. \tag{23}$$

3. NUMERICAL SETUP

Equations (20)–(22) are integrated outward from a small radius near the center. To avoid the central coordinate singularity, the integration starts at $\bar{r} = \bar{r}_0$ with the regular leading-order expansion

$$\bar{m}(\bar{r}_0) \simeq \frac{1}{3}\left(x_c^3 + y_c\right)\bar{r}_0^3. \tag{24}$$

The variables x and y are initialized at this radius by their central values. Integration is stopped when the baryonic and dark-matter components reach the chosen surface thresholds.

The baryonic central density is varied over the interval

$$\rho_{b,c} \in [10^6, 10^{11}]\ \mathrm{g\,cm^{-3}}. \tag{25}$$

The central dark-matter admixture is sampled through the representative set

$$\delta = 0,\ 0.25,\ 0.35, \tag{26}$$

where $\delta = 0$ corresponds to the standard Chandrasekhar sequence, while $\delta = 0.25$ and $\delta = 0.35$ represent two mixed cases with visibly stronger dark-matter contributions.

For each model we extract the total mass,

$$M = m(R), \tag{27}$$

the baryonic mass,

$$M_b = 4\pi \int_0^{R_b} r^2 \rho_b(r)\, dr, \tag{28}$$

and the dark-matter mass,

$$M_{dm} = 4\pi \int_0^{R_{dm}} r^2 \rho_{dm}(r)\, dr. \tag{29}$$

The final dark-matter mass fraction is

$$f_{dm} = \frac{M_{dm}}{M}. \tag{30}$$

We also define the limiting mass within the explored interval by

$$M_{lim}(\delta) = \max_{\rho_{b,c}} M(\rho_{b,c}; \delta). \tag{31}$$

This is only an operational readout over the scanned density range. It is not interpreted here as a complete dynamical stability limit.

For the representative mixed solution used in the density-profile analysis below, the integration starts at

$$\bar{r}_0 = 10^{-8}, \tag{32}$$

with the stopping thresholds

$$x_{\rm stop} = 10^{-6}, \qquad y_{\rm stop} = 10^{-6}. \tag{33}$$

The coupled equations are solved in *Mathematica* with the adaptive "StiffnessSwitching" method. The parameters used for Figure 1 are

$$\rho_{b,c} = 10^8 \ \mathrm{g\,cm^{-3}}, \qquad \delta = 0.25, \qquad \gamma = \frac{5}{3}, \qquad \alpha = 1. \tag{34}$$

4. RESULTS AND DISCUSSION

We now turn to the minimal set of outputs needed for the present purpose: density profiles, the mass–radius relation, and the limiting readout extracted from the explored sequences.

4.1. Density profiles

The radial structure is described by

$$\rho_b(r), \qquad \rho_{dm}(r), \qquad \rho_{tot}(r) = \rho_b(r) + \rho_{dm}(r). \tag{35}$$

A representative mixed model is sufficient to show how the dark component is distributed relative to the visible stellar matter and how it contributes to the total density profile.

Figure 1 displays the normalized density profiles $\rho_b/\rho_{b,c}$, $\rho_{DM}/\rho_{DM,c}$ and $\rho_{tot}/\rho_{tot,c}$ for the representative mixed configuration with $\rho_{b,c} = 10^8$ g cm^{-3}, $\delta = 0.25$, $\gamma = 5/3$ and $\alpha = 1$. The dark component is more centrally concentrated than the baryonic one and reaches zero at a smaller radius, $R_{DM} \approx 2101.81$ km, whereas the baryonic component extends to $R_b \approx 4169.29$ km. For this model

the total mass is $M \approx 1.01421\,M_\odot$, the dark-matter mass is $M_{DM} \approx 0.09843\,M_\odot$, and the corresponding mass fraction is $f_{DM} \approx 9.71 \times 10^{-2}$. This example illustrates that the dark component forms an inner compact region, while the visible stellar size remains determined by the baryonic surface.

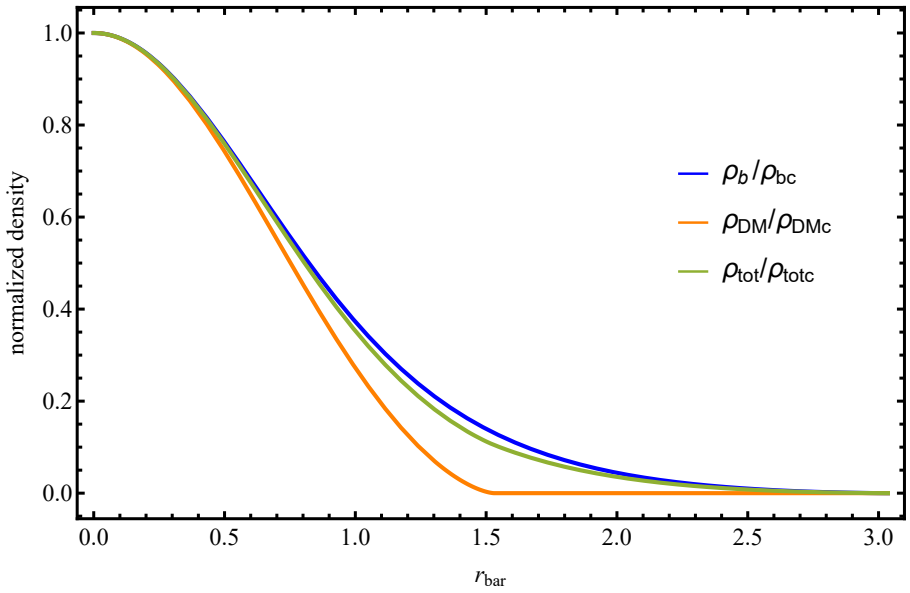

Figure 1 – Normalized density profiles $\rho_b/\rho_{b,c}$, $\rho_{DM}/\rho_{DM,c}$ and $\rho_{tot}/\rho_{tot,c}$ for the representative mixed model with $\rho_{b,c} = 10^8$ g cm^{-3}, $\delta = 0.25$, $\gamma = 5/3$ and $\alpha = 1$. The dark-matter profile decreases more rapidly with radius and terminates at $R_{DM} \approx 2101.81$ km, whereas the baryonic component extends to $R_b \approx 4169.29$ km.

4.2. Mass–radius relation

The main global quantity of interest is the mass–radius relation. In the present model the mass is the total gravitational mass obtained from Eq. (27) and the radius used for comparison is the baryonic radius R_b. Thus the relevant sequence is

$$M = M(R_b; \delta). \tag{36}$$

Figure 2 shows the mass–radius relation for the reference baryonic sequence ($\delta = 0$) together with two representative mixed cases, $\delta = 0.25$ and $\delta = 0.35$. For the mixed sequences, the numerical solutions were obtained over the central-density interval $\rho_{b,c} = 10^6$–10^8 g cm^{-3}, whereas the pure baryonic sequence was followed over the wider range $\rho_{b,c} = 10^6$–10^{11} g cm^{-3}. Within the explored interval, increasing the central dark-matter admixture shifts the mixed configurations toward lower masses and smaller baryonic radii relative to the standard Chandrasekhar sequence. This is already visible for the representative case $\rho_{b,c} = 10^8$ g cm^{-3}, where the total mass decreases from $1.18047\,M_\odot$ at $\delta = 0$ to $1.01421\,M_\odot$ at $\delta = 0.25$ and to $0.954212\,M_\odot$ at $\delta = 0.35$, while the baryonic radius decreases from 4327.58 km to 4169.29 km and 3843.33 km, respectively.

At a qualitative level, this shift is easy to understand. Once the dark component contributes to the common gravitational field, the baryonic structure responds to the total enclosed mass rather than to the baryonic mass alone. In this simple model, that is the basic mechanism behind the departure from the standard Chandrasekhar sequence.

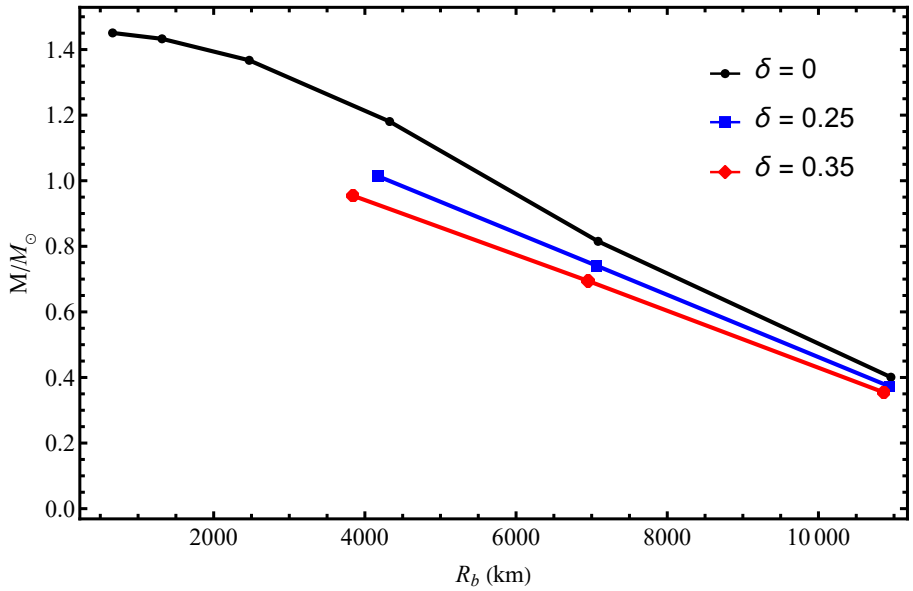

Figure 2 – Mass–radius relation $M/M_{\odot}$ versus R_b for the standard baryonic sequence ($\delta = 0$) and for two representative mixed configurations ($\delta = 0.25$ and $\delta = 0.35$). The mixed sequences are computed over the central-density range $\rho_{b,c} = 10^6$–10^8 g cm^{-3}, whereas the pure baryonic sequence extends to $\rho_{b,c} = 10^{11}$ g cm^{-3}. The mixed curves lie below the standard Chandrasekhar sequence, showing that an increasing dark-matter admixture reduces the total mass of the equilibrium configuration for the same general radius scale.

4.3. Relative impact of the dark-matter admixture

To quantify the influence of the dark component, we compare each mixed configuration with the purely baryonic model at the same central baryonic density. This comparison is useful because the parameter δ specifies only the central density ratio, whereas the final structural changes are determined by the integrated equilibrium solution. We therefore introduce the fractional changes in the total mass and in the baryonic radius as

$$\Delta M = \frac{M(\delta) - M(0)}{M(0)}, \qquad \Delta R = \frac{R_b(\delta) - R_b(0)}{R_b(0)}. \tag{37}$$

The resulting values are listed in Table 1. In the density interval where all three sequences are available, the dark-matter admixture systematically lowers the total mass and the baryonic radius. The mass reduction is already visible at $\rho_{b,c} = 10^6$ g cm^{-3} and becomes more pronounced as the central density increases. At $\rho_{b,c} = 10^8$ g cm^{-3}, the mass decreases by about 14.08% for $\delta = 0.25$ and by about 19.17% for $\delta = 0.35$. The corresponding decrease in the baryonic radius is about 3.66% and 11.19%, respectively.

This result gives a direct numerical measure of the effect of the dark component in the present minimal model. It also shows that the central admixture parameter δ should not be identified with the final dark-matter mass fraction. For example, at $\rho_{b,c} = 10^8$ g cm^{-3} the output mass fraction is $f_{DM} = 0.09705$ for $\delta = 0.25$, but it increases to $f_{DM} = 0.20760$ for $\delta = 0.35$. Thus, even for a fixed phenomenological dark-sector equation of state, the global importance of the dark component depends on the full equilibrium configuration, not only on the central input ratio.

Table 1. Relative changes of the mixed configurations with respect to the purely baryonic sequence at the same central baryonic density.

$\rho_{b,c}$ (g cm^{-3})	δ	$M/\mathrm{M}_\odot$	R_b (km)	f_{DM}	Δ_M	Δ_R
10^6	0.25	0.372661	10941.4	0.01936	-7.02%	-0.16%
10^6	0.35	0.354539	10864.5	0.03760	-11.54%	-0.86%
10^7	0.25	0.740940	7063.1	0.03330	-9.10%	-0.31%
10^7	0.35	0.694300	6953.5	0.06698	-14.82%	-1.86%
10^8	0.25	1.014210	4169.29	0.09705	-14.08%	-3.66%
10^8	0.35	0.954212	3843.33	0.20760	-19.17%	-11.19%

4.4. Limiting configurations

The largest masses obtained in the explored central-density interval are summarized through the limiting readout defined in Eq. (31). Together with the corresponding baryonic radius and dark-matter fraction, these values provide a compact comparison between the pure baryonic sequence and the representative mixed sequences.

Table 2. Limiting configurations within the explored central-density interval. For the mixed cases $\delta = 0.25$ and $\delta = 0.35$, the numerical scan was restricted to the range $\rho_{b,c} = 10^6$–10^8 g cm^{-3}. In these cases, the limiting quantities should be read as numerical outputs over the explored interval rather than as complete high-density maxima.

δ	$M_{\mathrm{lim}}/\mathrm{M}_\odot$	$R_{b,\mathrm{lim}}$ (km)	$f_{\mathrm{dm,lim}}$
0	1.45072	662.771	0
0.25	1.01421	4169.29	0.0970526
0.35	0.954212	3843.33	0.207596

The quantity f_{dm} is useful because the input parameter δ refers only to the central density ratio, whereas f_{dm} measures the final mass contribution of the dark component. In that sense, it gives a more direct estimate of how important the dark sector becomes in the resulting equilibrium configuration.

5. CONCLUSIONS

We have studied a minimal Newtonian model of a white dwarf containing a dark-matter admixture. The baryonic component was described by the Chandrasekhar equation of state, whereas the dark component was represented by an effective polytropic law. The two sectors were coupled only through the common Newtonian gravitational field. Within this deliberately restricted setup, the model provides a transparent baseline for comparing the standard Chandrasekhar sequence with mixed two-component configurations.

The numerical analysis focused on three simple but physically informative outputs: the density profiles, the mass-radius relation, and the limiting readout over the explored central-density interval. The density profiles show that, for the representative mixed configuration considered here, the dark component is more centrally concentrated than the baryonic component. The visible stellar boundary, however, remains determined by the baryonic surface.

A direct comparison at fixed central baryonic density shows that the dark-matter admixture produces a measurable reduction of both the total mass and the baryonic radius. At the reference density $\rho_{b,c} = 10^8$ g cm^{-3}, the mass decreases by about 14.08% for the case $\delta = 0.25$ and by about 19.17% for the case $\delta = 0.35$ relative to the purely baryonic configuration. The corresponding reductions in

the baryonic radius are about 3.66% and 11.19%, respectively. This result gives a direct quantitative measure of how strongly the central admixture parameter changes the global equilibrium sequence in the present model.

For the representative mixed configuration used in the density-profile analysis, we obtain $M \approx 1.01421\,M_\odot$, $R_b \approx 4169.29$ km, and $f_{DM} \approx 9.71 \times 10^{-2}$. This example illustrates that the dark component can form an inner compact region while the outer radius of the observable star is still set by the baryonic matter.

Within the explored central-density interval, increasing the central admixture from $\delta = 0$ to $\delta = 0.25$ and $\delta = 0.35$ moves the mixed configurations toward lower masses and smaller baryonic radii relative to the standard Chandrasekhar sequence. In particular, at $\rho_{b,c} = 10^8$ g cm^{-3} the total mass changes as $1.18047\,M_\odot$, $1.01421\,M_\odot$ and $0.954212\,M_\odot$ for the three cases, respectively.

The model remains intentionally limited. It does not include rotation, magnetic fields, finite-temperature corrections, general relativistic effects, or a specific microscopic dark-matter candidate. The results should therefore be interpreted as a baseline Newtonian calculation rather than as a complete astrophysical model of dark-matter-admixed white dwarfs. Nevertheless, the calculation shows that even this minimal two-component framework is able to isolate the structural role of an additional gravitating component and to quantify its impact on the white-dwarf equilibrium sequence.

REFERENCES

1. Bertone, G., D. Hooper, and J. Silk, "Particle dark matter: Evidence, candidates and constraints." 279–390, 2005.
2. Aghanim, N., Y. Akrami, M. Ashdown, J. Aumont, and C. Baccigalupi. "Planck 2018 results. vi. cosmological parameters." *Astron. Astrophys.* 641 (2020): A6. https://doi/org/10.1051/0004-6361/201833910
3. Rubin, V. C. and W. K. Ford Jr. "Rotation of the andromeda nebula from a spectroscopic survey of emission regions." *Astrophysical Journal, vol. 159, p. 379* 159 (1970): 379.
4. Bertone, G. and M. Fairbairn. "Compact stars as dark matter probes." *Physical Review D—Particles, Fields, Gravitation, and Cosmology* 77, no. 4 (2008): 043515.
5. Kouvaris, C. and P. Tinyakov. "Can neutron stars constrain dark matter?" *Physical Review D—Particles, Fields, Gravitation, and Cosmology* 82, no. 6 (2010): 063531.
6. Bramante, J. and N. Raj. "Dark matter in compact stars." *Physics Reports* 1052 (2024): 1–48.
7. Chandrasekhar, S. "The maximum mass of ideal white dwarfs." *Astrophysical Journal, vol. 74, p. 81* 74 (1931): 81.
8. Chandrasekhar, S. *An Introduction to the Study of Stellar Structure*. Chicago: University of Chicago Press, 1939.
9. Hamada, T. and E. E. Salpeter. "Models for zero-temperature stars." *The Astrophysical Journal* 134 (1961): 683–698.
10. Shapiro, S. L. and S. A. Teukolsky. *Black Holes, White Dwarfs, and Neutron Stars: The Physics of Compact Objects*. New York: Wiley-Interscience, 1983.
11. Kippenhahn, R., A. Weigert, and A. Weiss. *Stellar Structure and Evolution*. Berlin: Springer, 2013.
12. Orazymbet, A., A. Muratkhan, D. Utepova, N. Beissen, G. Baimbetova, and S. Toktarbay. "Numerical solutions and stability analysis of white dwarfs with a generalized anisotropic factor." *Galaxies* 13, no. 3 (2025): 69. https://doi.org10.3390/galaxies13030069
13. Leung, S.-C., M.-C. Chu, L.-M. Lin, and K.-W. Wong. "Dark-matter admixed white dwarfs." *Physical Review D* 87, no. 12 (2013): 123506.
14. Chan, H.-S., M.-C. Chu, and S.-C. Leung. "Dark matter-admixed rotating white dwarfs as peculiar compact objects." *The Astrophysical Journal* 941, no. 2 (2022): 115.
15. Carvalho, G. A., J. D. V. Arbañil, and J. G. Coelho. "Effects of light-mass fermionic dark matter on the equilibrium and stability of white dwarfs." *Physical Review D* 112 (2025): 044047.
16. Nunes, S. P., J. D. V. Arbañil, J. M. Z. Pretel, and S. B. Duarte. "Dark matter in white dwarfs: Implications for their structure." *Journal of High Energy Astrophysics* 50 (2026): 100505.
17. Sahoo, R., S. Mukhopadhyay, and M. Bhuyan. "Dark matter admixed white dwarfs: A single-fluid approach." *arXiv preprint arXiv:2511.17120* (2025):
18. Salpeter, E. E. "Energy and pressure of a zero-temperature plasma." *The Astrophysical Journal* 134 (1961): 669–682.

19. Horedt, G. P. *Polytropes: applications in astrophysics and related fields*. Springer, 2004.
20. Glendenning, N. K. *Compact Stars: Nuclear Physics, Particle Physics, and General Relativity*. New York: Springer, 2000.
21. Graham, P. W., R. Janish, V. Narayan, S. Rajendran, and P. Riggins. "White dwarfs as dark matter detectors." *Physical Review D* 98 (2018): 115027.
22. Bell, N. F., G. Busoni, M. E. Ramirez-Quezada, S. Robles, and M. Virgato. "Improved treatment of dark matter capture in white dwarfs." *Journal of Cosmology and Astroparticle Physics* 10 (2021): 083.
23. Hoefken Zink, J., S. Hor, and M. E. Ramirez-Quezada. "Dark matter interactions in white dwarfs: A multi-energy approach to capture mechanisms." *Journal of High Energy Physics* 05 (2025): 160.

Information about authors

Arailym Muratkhan *– PhD, Senior Lecturer, Department of Theoretical and Nuclear Physics, Al-Farabi Kazakh National University, Almaty, Kazakhstan, email: muratkhan.aray@kaznu.kz,*

Nurikamal Shynggyskhan *– PhD student of the 3rd year of the specialty «8D05306 – Physics», Department of Theoretical and Nuclear Physics, Al-Farabi Kazakh National University, Almaty, Kazakhstan, e-mail: nurkamal8503@gmail.com ,*

Saken Toktarbay *– PhD, Professor, Department of Theoretical and Nuclear Physics, Al-Farabi Kazakh National University, Almaty, Kazakhstan, e-mail: saken.toktarbay@kaznu.edu.kz.*